

Lattice instability in the solid-state amorphization of Fe(Al) solid solutions by mechanical alloying

H. W. Sheng, Y. H. Zhao, Z. Q. Hu, and K. Lu

State Key Laboratory for RSA, Institute of Metal Research, Chinese Academy of Sciences, Shenyang 110015, People's Republic of China

(Received 24 March 1997)

Metastable $\text{Fe}_{100-x}\text{Al}_x$ alloys have been formed by ball milling of elemental Fe and Al powders: supersaturated body-centered-cubic solid solutions for $x \leq 70$, and an amorphous phase for $x > 70$. Quantitative x-ray-diffraction measurements show that the total root-mean-square displacement (rms) and the static rms in the $\text{Fe}_{100-x}\text{Al}_x$ solid solutions increase significantly with increasing Al content. The total rms at the instability point, however, reaches only 6.8% of the nearest-neighbor distance and is far below the critical value predicted by the Lindemann melting criterion, suggesting that the Lindemann melting criterion is not applicable for the solid-state amorphization. Instead, the Debye temperature of the supersaturated $\text{Fe}_{100-x}\text{Al}_x$ alloys was observed to drop by $\sim 22\%$ at the point of amorphization, implying a corresponding softening in the average shear modulus of $\sim 40\%$, which agrees with the microhardness measurements. These results strongly support the empirical elastic instability criterion for the solid-state amorphization process. [S0163-1829(97)05129-1]

Currently, the crystalline-to-amorphous phase transformation (i.e., amorphization) receives considerable scientific interest, because it is related to ordinary melting as both phenomena represent a periodic-to-aperiodic phase transformation.¹⁻⁴ Experimentally, solid-state amorphization can be induced by a variety of techniques.⁵ All of the processes have in common the fact that they lead to static disordering of the parent crystalline phase by the incorporation of nonequilibrium defects. Due to the incorporated atomic disorder, the crystalline phase is driven into an instability at which the crystalline collapses into an amorphous phase.

Yet today we are not in a consensus about the lattice instability which constitutes the ultimate limit of the defective crystals. There are several lattice instability models proposed to account for amorphization, which are either vibrational,³ elastic,⁶⁻⁸ topological⁹ or entropical.¹⁰ Among them, the elastic instability criterion assumes that amorphization takes place when the atomic disorder created in the lattice causes the softening of the elastic constant to a critical value.⁶⁻⁸ More recently, Lam and Okamoto have proposed a unified approach to solid-state amorphization based on a generalized form of the Lindemann melting criterion (see, for details, Ref. 4). These models, however, were established on the basis of limited experimental evidence (mainly from irradiation and implantation investigations), the question of the general reliability of them still remains.

In a binary system, extended solid solutions are often formed by rapid quenching, vapor quenching, and mechanical alloying. If the crystalline solid solution is maintained in a polymorphous configuration, it can be driven to the amorphous state by supersaturating it beyond a certain concentration. Therefore, these alloy systems offer unique materials to test the underlying mechanism of amorphization. Nevertheless, such attempts were scarcely reported before. Recently, Krill *et al.*¹¹ investigated the precursor effect of amorphization in a Nb-Pd binary alloy. Their measurements, however, failed to reach the critical point at which the amorphization takes place. In this paper, we will report the amorphization of binary Fe-Al solid solutions by mechanical alloying. Fur-

ther, the atomic vibration properties and Debye temperature of the bcc structured Fe-Al will be systematically measured by means of x-ray diffraction, in order to check the Lindemann melting criterion vs the elastic instability criterion for solid-state amorphization.

Mechanical alloying of a mixture of pure Fe powder (99.9%, 100 mesh) and pure Al powder (99.999%, 200 mesh) was carried out in a planetary ball mill with stainless-steel balls and vial at ambient temperature. The ball-to-powder weight ratio was 20:1 and 10 g of mixed powder was used for each run. The loaded vial was sealed in dry Ar with an overpressure about 2 atm. The milling process was not interrupted for 150 h. The overall powder compositions were varied between 0 and 80 at % Al. In all the cases, wet chemical analysis and energy-dispersive x-ray analysis indicated the impurity level of less than 500 ppm and 1 at % Fe in the final milled products.

The as-prepared samples were studied by x-ray diffraction (XRD) on a Rigaku DMAX/2400 x-ray diffractometer operated at 150 mA, 50 kV with Cu $K\alpha$ radiation. The diffractometer was equipped with a low-temperature attachment, which allows the quantitative measurement in a temperature range from 88 to 295 K. Measurements of $\theta \sim 2\theta$ scans were made in the reflection mode. Small angular steps of $2\theta = 0.02^\circ$ and a fixed counting time of 5 s were taken to measure the intensity of each Bragg reflection.

For microhardness measurements, the alloyed powders were embedded in epoxy and mechanically polished. Microhardness was measured in a MVK-H3 microhardness tester at a load of 10 gf. At least ten measurements for each sample were collected to calculate the average values.

XRD patterns indicate that metastable $\text{Fe}_{100-x}\text{Al}_x$ phases were obtained after ball milling, as qualitatively shown in Fig. 1. For $x \leq 70$, all the bcc Fe peaks consistently shifted to lower angles compared with the peaks for the as-milled pure Fe peaks, and no indication of the Al (or other) phase can be identified. This indicates the formation of a Fe-based bcc solution supersaturated with Al solutes. For $x > 70$, in con-

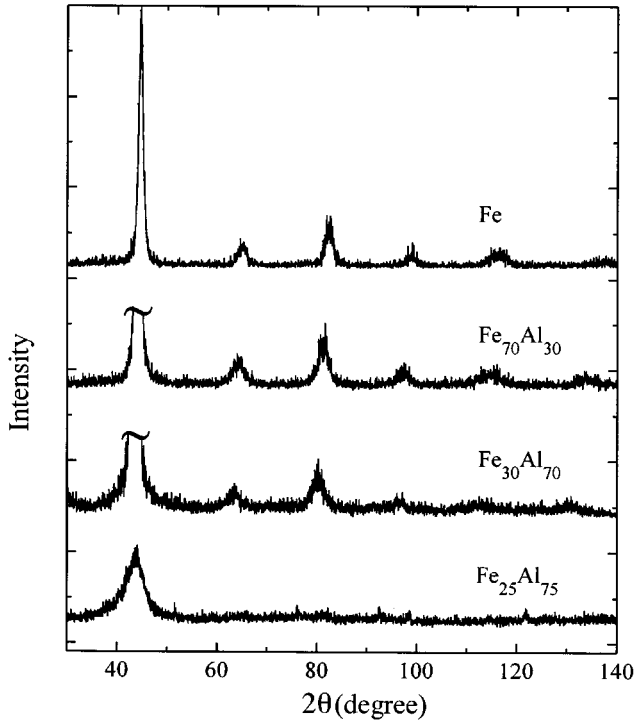


FIG. 1. XRD patterns showing the formation of Fe-Al supersaturated solutions ($x \leq 70$) and amorphous phase ($x > 70$) by mechanical alloying pure Fe and Al powders for 150 h.

trast, broad halos indicative of amorphous phase formation become the main feature in the diffraction spectra and all the crystalline Bragg peaks fade away. In fact, the nature of the amorphous $\text{Fe}_{20}\text{Al}_{80}$ has been previously examined by Mössbauer spectroscopy.¹² It is clear that, the mechanically driven amorphization of Fe-Al solutions had taken place when the Al concentration reached a critical value $x^* = 70$. Since no phase separation was observed in the Fe-Al system upon milling, the amorphization meets the polymorphous constraints, which favors the quantitative x-ray-diffraction study of the crystalline-to-amorphous transformation.

Figure 2(a) shows the lattice parameter of Fe-Al solutions as determined by Nelson-Riley plot analysis.¹³ The lattice parameter, a_0 , increases monotonically as a function of Al concentration, suggesting the formation of the $\text{Fe}_{100-x}\text{Al}_x$ solid solution. At the instability point ($x^* = 70$), a maximum increase of the lattice parameter was found to be $\Delta a/a_0 = 2.7\%$, which corresponds an increase in the atomic volume by 8.3%. From the XRD line broadening, the grain size and homogeneous microstrain in the as-prepared Fe-Al solutions can be obtained by using the Scherrer and Wilson equation,¹⁴ as demonstrated in Fig. 2(b). One may find that the grain size for all the Fe-Al solutions lies in the range of 5–8 nm and slightly changes with the composition. On the contrary, the microstrain continuously increases up to 0.17% with the incorporation of Al solutes up to $x^* = 70$.

In order to explore the mechanism of the solid-state amorphization, the atomic vibration properties of the Fe-Al solutions have been measured. For a random solid solution, due to the atomic vibration, the intensities of Debye-Scherrer lines will be attenuated by the Debye-Waller factor,¹⁵ $\exp(-2M)$. Under a reasonable assumption that Fe and Al have equal mean-square displacement (msd),¹¹ $\langle u_{\text{tot}}^2 \rangle$, it can

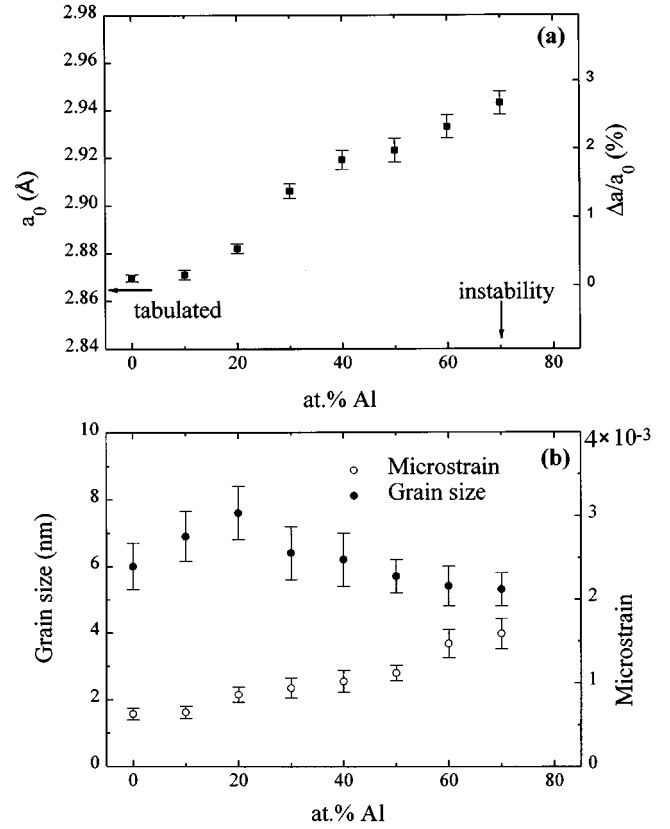


FIG. 2. (a) The lattice parameter and (b) the grain size and homogeneous microstrain of the bcc solid solution as a function of Al concentration.

be shown that $\langle u_{\text{tot}}^2 \rangle$ is related to M according to the expression:

$$M = 8 \pi^2 \langle u_{\text{tot}}^2 \rangle (\sin \theta / \lambda)^2, \quad (1)$$

where λ is the wave length of the x ray, θ is the Bragg angle. Thus, by determining the Debye-Waller factor from the x-ray-diffraction scans taken at different temperatures and compositions, the composition dependence of $\langle u_{\text{tot}}^2 \rangle$ can be measured. Since the atomic vibration contains two parts, i.e., the static and the thermal one, as expressed by

$$\langle u_{\text{tot}}^2 \rangle = \langle u_{\text{sta}}^2 \rangle + 3 \hbar^2 F(y) / M_a k_B \Theta, \quad (2)$$

where $\langle u_{\text{sta}}^2 \rangle$ contains any static displacements in the material, M_a is the atomic mass, k_B is the Boltzmann constant, Θ is the Debye temperature, $y = \Theta/T$, and

$$F(y) = \frac{1}{4} + \frac{1}{y^2} \int_0^y \frac{\zeta d\xi}{\exp(\xi) - 1},$$

the parameter $\langle u_{\text{sta}}^2 \rangle$ and Θ can be obtained by fitting $\langle u_{\text{tot}}^2 \rangle$ at several temperatures to Eq. (2).

Figure 3 illustrates the rapid increase in both $\langle u_{\text{tot}}^2 \rangle^{1/2}$ and $\langle u_{\text{sta}}^2 \rangle^{1/2}$ with increasing supersaturation of the bcc phase. It is obvious that, in Fe-Al disordered crystals, atomic disorder creates significant static displacements. A similar composition dependence of $\langle u_{\text{sta}}^2 \rangle^{1/2}$ was observed by Krill *et al.*¹¹ in the Nb-Pd binary-alloy system.

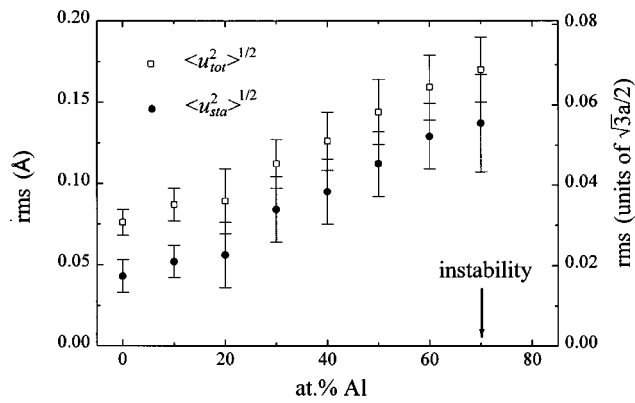


FIG. 3. Total and static root-mean-square displacements versus Al concentration.

The Lindemann melting criterion predicts that melting of a crystalline solid will occur when the atomic root-mean-square displacement (rms) reaches a critical fraction of the nearest-neighbor distance.¹⁶ Voronel *et al.*¹⁷ recently demonstrated that the Lindemann criterion holds for alloys if the total msd, rather than only the dynamic msd, is used to predict the melting point. That is, $\langle u_{sta}^2 \rangle$ plays an equivalent role to $\langle u_{vib}^2 \rangle$ in influencing the melting temperature of alloys. As to the solid-state amorphization, it is assumed that the Lindemann melting criterion is also applicable due to the significant static displacements in addition to displacements resulting from thermal vibration.⁴ In the present case of Fe_{100-x}Al_x alloys, the rms increases rapidly with the Al concentration. When the solid-state amorphization occurs at $x^* = 70$, the total rms of the solid solution reaches 0.169 Å, which is about 6.8% of the nearest-neighbor distance. Evidently, this value is far below the critical value as predicted by Lindemann criterion for the melting of the bcc elements (15%). Actually, it has been found in previous studies that the observed average total rms before the onset of amorphization is often less than the value predicted by the Lindemann melting criterion, such as thin Al films implanted with Mn (Ref. 19) and B-ion implantation into Nb.²⁰ Therefore, it seems that the Lindemann melting criterion does not hold for the solid-state amorphization, even though there are some parallels between these two phenomena.

An alternative interpretation to the solid-state amorphization of Fe-Al is the elastic modulus softening. The atomic disorder created in the crystalline lattice in the form of static atomic displacement would lead to the softening of the shear elastic modulus due to the elastic anharmonicity. It has been empirically shown that a drop in the Debye temperature by ~20% and corresponding softening in the average shear modulus G of more than 40% were observed at the point of amorphization, where the average shear modulus of the defective crystal becomes equal to the amorphous phase.^{4,21} This phenomenon has been confirmed by a body of molecular-dynamic simulations.²²⁻²⁴ In the present case, the Debye temperature of Fe-Al solid solutions has been measured according to Eq. (2), as shown in Fig. 4(a). The Debye temperature decreases with increasing Al content. Up to $x = 70$, the maximum drop in Θ measured in Fe-Al alloys is ~22%. In analogy with the analysis of Ettl and Samwer,²¹ it was found that this value corresponds to a decrease in G of

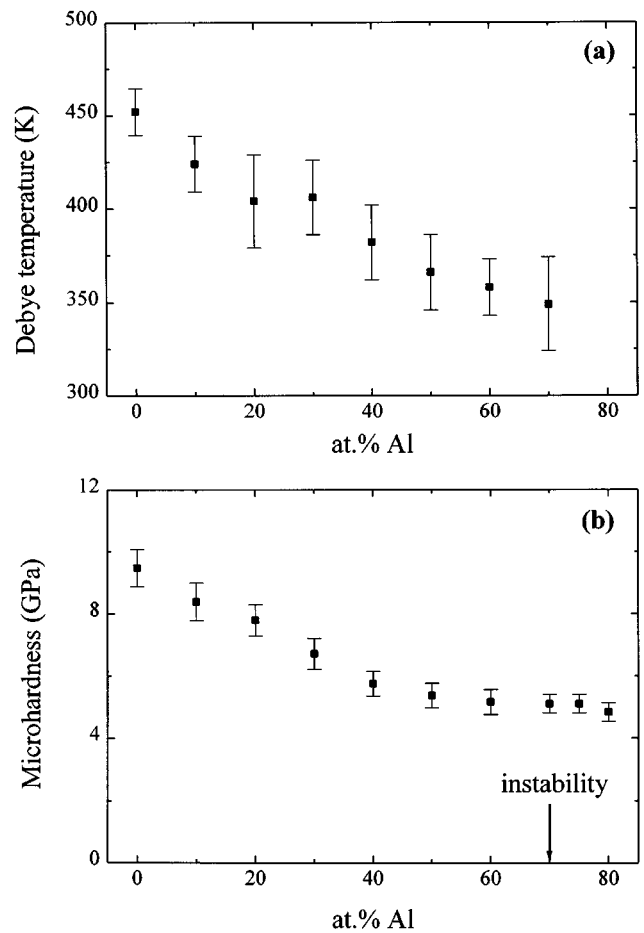


FIG. 4. (a) Debye temperature Θ plotted against Al concentration for Fe-Al compositions derived from x-ray-diffraction measurements. (b) Variation of the microhardness for as-prepared Fe-Al solid solutions with different Al concentrations, indirectly showing the elastic modulus softening.

about 40%, which is in a qualitative agreement with the empirical value of the change in the shear elastic constant at the instability point.

The elastic modulus softening as an indication of the solid-state amorphization is also evidenced from the microhardness decrease. Figure 4(b) shows the variation of microhardness of Fe-Al as a function of Al content. One may find that the microhardness decreases with increasing Al content and approaches that of the amorphous phase. At the instability point, the microhardness decreases by ~50%. The “solid-solution softening” phenomenon has been previously found in other alloy systems.^{25,26} It is known that the microhardness is relevant to the elastic modulus as well as the grain size of the sample. Provided that the grain size is the same for all the samples, the microhardness scales with the elastic modulus according to the Hall-Petch relation.²⁷ In turn, the microhardness would measure the elastic modulus of the material. Since the grain sizes of Fe-Al samples involved in the present study are slightly changed, the size effect on the microhardness can be reasonably ignored, that is, the microhardness decrease might be caused by the elastic modulus softening effect. The amorphization sets in when the microhardness, or elastic modulus, falls to the value of the amorphous phase as seen from Fig. 4(b). Hence, it is

inevitable that the elastic instability criterion might be the underlying mechanism for the solid-state amorphization in the Fe-Al alloy system.

In summary, we have realized the solid-state amorphization in Fe_{100-x}Al_x alloys, and measured the atomic vibration properties for the supersaturated solid solutions. The rms amplitude of atoms was found to increase rapidly with the incorporation of Al atoms. The total rms of Fe_{100-x}Al_x at the point amorphization is far below the critical value predicted by the Lindemann melting criterion, implying that the Lindemann melting criterion does not hold for the solid-state amorphization. The measured Debye temperature of

Fe_{100-x}Al_x solid solutions decreases by ~22% prior to amorphization. This value corresponds to a softening in average shear modulus by ~40% and coincides well with previous findings. The softening of the shear elastic modulus is also evidenced from the microhardness measurements. It is thus suggested the elastic instability criterion might be the underlying mechanism for the solid-state amorphization.

The authors would like to thank Professor S. Z. Lin for helpful discussions. Financial support from the Chinese Academy of Sciences and the National Science Foundation of China (Grant No. 59625101) are acknowledged.

-
- ¹ W. L. Johnson, M. Li, and C. E. Krill III, *J. Non-Cryst. Solids* **156/158**, 481 (1993).
- ² D. Wolf, P. R. Okamoto, S. Yip, J. F. Lutsko, and M. Kluge, *J. Mater. Res.* **5**, 286 (1990).
- ³ H. J. Fecht and W. L. Johnson, *Mater. Sci. Eng. A* **133**, 427 (1991).
- ⁴ N. Q. Lam and P. R. Okamoto, *MRS Bull.* **19**, 41 (1994).
- ⁵ W. L. Johnson, *Prog. Mater. Sci.* **30**, 81 (1986).
- ⁶ L. E. Rehn, P. R. Okamoto, J. Pearson, R. Bhadra, and M. Grimsditch, *Phys. Rev. Lett.* **59**, 2987 (1987).
- ⁷ J. L. Tallon, *Nature (London)* **342**, 658 (1989).
- ⁸ J. Koike, *Phys. Rev. B* **47**, 7700 (1993).
- ⁹ T. Egami and Y. Waseda, *J. Non-Cryst. Solids* **64**, 113 (1984).
- ¹⁰ H. J. Fecht and W. L. Johnson, *Nature (London)* **334**, 50 (1988).
- ¹¹ C. E. Krill III, J. Li, C. M. Garland, C. Ettl, K. Samwer, W. B. Yelon, and W. L. Johnson, *J. Mater. Res.* **10**, 280 (1995).
- ¹² Y. D. Dong, W. H. Wang, L. Liu, K. Q. Xiao, S. H. Tong, and Y. Z. He, *Mater. Sci. Eng. A* **134**, 867 (1991).
- ¹³ J. B. Nelson and D. P. Riley, *Proc. Phys. Soc. London* **57**, 160 (1945).
- ¹⁴ H. P. Klug and L. E. Alexander, *X-ray Diffraction Procedures for Polycrystalline and Amorphous Materials*, 2nd ed. (Wiley, New York, 1974), p. 662.
- ¹⁵ B. E. Warren, *X-ray Diffraction* (New York, Dover, 1990).
- ¹⁶ F. A. Lindemann, *Z. Phys.* **11**, 609 (1910).
- ¹⁷ A. Voronel, S. Rabinovich, A. Kisliuk, V. Steinberg, and T. Sverbilova, *Phys. Rev. Lett.* **60**, 2402 (1988).
- ¹⁸ S. A. Cho, *J. Phys. F* **12**, 1069 (1982).
- ¹⁹ A. Seidel, S. Massing, B. Strehlau, and G. Linker, *Phys. Rev. B* **38**, 2273 (1988).
- ²⁰ G. Linker, *Nucl. Instrum. Methods Phys. Res. B* **19/20**, 526 (1987).
- ²¹ C. Ettl and K. Samwer, *J. Non-Cryst. Solids* **156-158**, 502 (1993).
- ²² N. Q. Lam, P. R. Okamoto, M. J. Sabochick, and R. Devanathan, *J. Alloys Compd.* **184**, 429 (1993).
- ²³ R. Devanathan, N. Q. Lam, P. R. Okamoto, and M. Meshii, *Phys. Rev. B* **48**, 42 (1993).
- ²⁴ M. Li and W. L. Johnson, *Phys. Rev. Lett.* **70**, 1120 (1993).
- ²⁵ M. Zhu and H. J. Fecht, *Nanostruct. Mater.* **6**, 421 (1995).
- ²⁶ T. D. Shen and C. C. Koch, *Acta Mater.* **44**, 753 (1996).
- ²⁷ R. W. Armstrong, *Yield, Flow and Fracture of Polycrystals* (Applied Science, Cambridge, 1983).